Fully Chitosan-Based Thermoresponsive Hydrogel for Efficient Cu^{2+} Adsorption and Regeneration

Xiaohan Zha [a,b,#] Zhuoying Meng [a,#] Chen Wang,[a,b] Yiwen Ye,[a,b] Jiale Zhou,[a,b] Ruilin Zhang,[a,b] Jingyuan Li,[a,b] Shifeng Ma,[a,b] Chengyu Tan,[a,b,*] and Ye Tian [a,b,c,*]

To efficiently remove Cu^{2+} from wastewater, a fully chitosan thermoresponsive hydrogel (IPS_{gel}) was prepared using chitosan as the raw material. IPS_{gel} exhibited pronounced thermoresponsive behavior as well as a high adsorption capacity toward Cu^{2+}. When the temperature exceeded its volume phase transition temperature (VPTT = 35.4 °C), enhanced hydrophobic interactions among with the alkyl groups along the polymer chains induced rapid dehydration, shrinkage, and a reversible volume phase transition. The effects of initial Cu^{2+} concentration and pH on adsorption performance were systematically evaluated. The adsorption process followed the Langmuir isotherm and pseudo-second-order kinetic models, and a maximum adsorption capacity of 24.5 g/g was achieved. During regeneration, only 0.23 L of 0.1 M hydrochloric acid per gram of IPS_{gel} was required for rapid Cu^{2+} desorption, representing a reduction of approximately 88 to 95% compared to the conventional acid consumption (2 to 5 L/g) of traditional hydrogels. These findings indicate that by integrating thermoresponsiveness, high adsorption capacity, and efficient regeneration, the chitosan-based IPS_{gel} shows strong potential for wastewater treatment applications and provides a new strategy for the green design of purification materials.

DOI: 10.15376/biores.21.3.8001-8014

Keywords: Chitosan; Thermoresponsive; Hydrogel; Cu^{2+} adsorption; Reusability

Contact information: a: Key Laboratory of Environment Controlled Aquaculture, Dalian Ocean University, Ministry of Education, Dalian 116023, China; b: College of Marine Science and Environment, Dalian Ocean University, Dalian 116023, China; c: College of Biosystems Engineering and Food Science (BEFS), Zhejiang University, Hangzhou 310058, China; #: Xiaohan Zha and Zhuoying Meng contributed equally to the work, they are jointly listed as first authors;
** Corresponding author: tianye@dlou.edu.cn; tanchyu@dlou.edu.cn*

INTRODUCTION

Chitosan, a natural polysaccharide derived from chitin, is the only basic polysaccharide found in nature. It has high biological activity and economic value, so it can be used as a biomedical material, an aquatic feed additive, or an industrial wastewater treatment material (Arafa *et al.* 2024; Zha *et al.* 2026). However, one notable thing about chitosan is that it dissolves in acidic solutions but not in alkaline ones. This limits how it can be processed and makes it more difficult to prepare chitosan-based materials (Crini and Lichtfouse 2019; Nankawa *et al.* 2025). Therefore, exploring and optimizing chitosan processing strategies is both theoretically important and practically useful.

Industrial wastewater containing copper ions is commonly discharged into the environment, and the potential hazards of this pollutant cannot be overlooked. Excessive Cu^{2+} can be readily adsorbed by soils and sediments, subsequently accumulating through

the food chain and ultimately entering the human body (Zhen *et al.* 2022). The long-term intake of Cu^{2+}-contaminated food may lead to chronic toxicity, causing irreversible damage to multiple organs, including the respiratory and digestive systems (Jeremias *et al.* 2023; Sahu *et al.* 2025). Moreover, exposure to Cu^{2+} may increase carcinogenic risks. Common wastewater treatment methods for the removal of Cu^{2+} include adsorption, ion exchange, chemical precipitation, and membrane filtration (Cai *et al.* 2024). Among these, adsorption is considered an efficient and promising approach due to its operational simplicity, low cost, and ease of regeneration (Chen *et al.* 2025). In recent years, hydrogel-based adsorbents have attracted significant attention for heavy metal removal because of their three-dimensional network structure, hydrophilicity, and tunable functionality (Chen *et al.* 2022). In particular, natural polysaccharide-based hydrogels, such as those derived from chitosan, exhibit excellent biocompatibility and biodegradability. The abundant amino and hydroxyl groups of these hydrogels serve as effective binding sites, enabling coordination interactions with Cu^{2+} that provide enhanced adsorption capacity and selectivity (Badsha *et al.* 2021; Khan *et al.* 2021).

However, challenges, such as difficult recovery, potential secondary pollution, and insufficient cycling stability, have limited the practical application of hydrogel-based adsorbents. Moreover, conventional desorption methods typically rely on large volumes of concentrated acidic eluents, leading to high operational costs and severe secondary pollution. There is a need to develop environmentally friendly alternatives (De Luna *et al.* 2015; Park and Lee 2022; Zhi *et al.* 2025). To address the above challenges, stimulus-responsive hydrogels, particularly thermoresponsive systems, have emerged as promising alternatives for adsorbent recovery and reuse. These materials undergo reversible swelling–shrinkage transitions when the environmental temperature crosses the volume phase transition temperature (VPTT) (Sun *et al.* 2024; Wang *et al.* 2025), enabling mild regeneration and the efficient release of adsorbed pollutants (Suljovrujic *et al.* 2019; Zhi *et al*. 2025).

Based on these considerations, a fully chitosan thermoresponsive hydrogel was developed in this study for the efficient removal of Cu^{2+}. Chitosan was first treated *via* an alkaline dissolution method and subsequently modified to obtain thermoresponsive, 2-hydroxy-3-isopropoxypropyl chitosan (hereafter denoted as IPS).. This approach endowed the chitosan with temperature sensitivity while also improving its solubility, thereby enhancing its processability.

Subsequently, IPS was employed as the sol-gel framework to construct a molecularly functionalized thermoresponsive hydrogel (denoted as IPS_{gel}) through a covalent crosslinking strategy, enabling improved Cu^{2+} adsorption performance. The structure and morphology of the hydrogel were characterized by Fourier transform infrared spectroscopy (FTIR) and scanning electron microscopy (SEM). Then, the thermoresponsive swelling–shrinkage behavior of IPS_{gel} was systematically investigated. Considering the prospective application of this material in saline wastewater, NaCl was used as an example to observe how the ionic environment affects the thermosensitive behavior of the hydrogel. The introduction of salt ions competes with hydrophilic groups for water molecules, weakens hydrogen bonding, and allows hydrophobic interactions to gradually dominate, thereby lowering the VPTT of the hydrogel. In addition, pH significantly alters the existing forms and adsorption properties of Cu^{2+} in solution. Therefore, this work considered the effect of pH on the adsorption capacity and identified the optimal pH condition, under which all subsequent adsorption isotherm and kinetic experiments were carried out. These results p.rovide a reference for understanding how

ions and pH synergistically regulate the adsorption process. Effects of pH (1.5 to 6.0) and Cu^{2+} concentration (25 to 200 mg/L) were studied relative to the Cu^{2+} adsorption capacity. The adsorption process was analyzed using isotherm models (Langmuir and Freundlich) and kinetic models (pseudo-first-order and pseudo-second-order). In addition, the reusability and regeneration performance of IPS_{gel} were comprehensively assessed.

EXPERIMENTAL

Materials

Isopropyl glycidyl ether (IPGE), ethylene glycol diglycidyl ether (EDGE), and lithium hydroxide (LiOH, analytical grade) were obtained from Tokyo Chemical Industry Co., Ltd. (Tokyo, Japan). Anhydrous copper sulfate ($CuSO_4$, analytical grade) was purchased from Tianjin Damao Chemical Reagent Factory (Tianjin, China). Potassium hydroxide (KOH, analytical grade) and chitosan (degree of deacetylation ≥ 95%, viscosity 100 to 200 mPa·s) were obtained from Aladdin Biochemical Technology Co., Ltd. (Shanghai, China). Sodium hydroxide (NaOH, analytical grade) was supplied by Sinopharm Chemical Reagent Co., Ltd. (Shanghai, China).

Methods

Synthesis of thermoresponsive IPS_{gel}

A mixed aqueous solution containing 4.5 wt% LiOH, 4.5 wt% KOH, and 3.5 wt% urea was first prepared. Chitosan (CS) was then added to achieve a concentration of 2.8 wt%, followed by continuous stirring. This mixture was frozen at −40 °C for 3 h to obtain a transparent CS solution. Subsequently, the pH of the solution was adjusted to approximately 12 by adding 1M NaOH, and the mixture was heated in a 60 °C water bath with stirring for 1 h. The IPGE was then introduced, and the reaction was maintained for 5 h. The product was purified by dialysis for 72 h, followed by rotary evaporation and freeze-drying to obtain purified IPS. The obtained IPS powder was redissolved, and NaOH was added until complete dissolution was achieved. The EDGE was slowly added in a 45 °C water bath to form the hydrogel *via* covalent crosslinking. The swelling–shrinkage behavior of this hydrogel was repeatedly evaluated using deionized water at 22 °C and 40 °C. Finally, the hydrogel was freeze-dried to obtain dried IPS_{gel} (Dai *et al.* 2022; Zha *et al.* 2026).

Morphological and structural characterization of IPS_{gel}

Fourier transform infrared spectra of CS, IPS, and IPS_{gel} were recorded in the range of 800 to 4000 cm^{-1} using an IRTracer-100 spectrometer (Shimadzu, Japan). For morphological analysis, the surfaces of dried shrunken and swollen IPS_{gel} samples were sputter-coated with gold prior to observation. The SEM images were obtained using a JSM-7800F field emission scanning electron microscope (JEOL, Japan).

Swelling properties of IPS_{gel}

The swelling behavior of IPS_{gel} was investigated using a gravimetric method. Dried IPS_{gel} samples (200 mg) were immersed in deionized water at a temperature of 22 °C for 24 h to reach swelling equilibrium. The IPS_{gel} samples were then transferred to a 40 °C water bath for 15 min to induce shrinkage. After removing excess surface water, the samples were weighed. This process was repeated several times to ensure reproducibility.

To evaluate the effect of ionic strength on the VPTT, NaCl solutions with concentrations of 0, 4, 8, 12, and 20 g/L were used. The swelling ratio (SR) (Zha *et al*. 2026) of IPS_{gel} was calculated according to Eq. 1,

$$SR\ (g/g) = (W_t\text{-}W_d)/W_d \quad (1)$$

where W_t is the weight (g) of the IPS_{gel} sample (including all water in the system after immersion) and W_d is the weight (g) of the dried IPS_{gel}.

Cu^{2+} adsorption capacity of IPS_{gel}

Adsorption experiments were conducted by adding IPS_{gel} (15 mg) to Cu^{2+} aqueous solutions. The solution pH was adjusted to 6.0 using 0.1 M HCl or NaOH, and an incubator shaker (300 rpm, 22 °C) was employed for 4 h to achieve adsorption equilibrium. The residual concentration of Cu^{2+} in each solution was determined by atomic absorption spectroscopy (USA -Perkin Elmer-AAnalyst 400).

To investigate the effect of pH on adsorption performance, Cu^{2+} solutions (100 mg/L) with pH values of 1.5 to 6.0 were prepared using 0.1 M HCl and NaOH. The adsorption capacity of IPS_{gel} for Cu^{2+} was calculated using Eq. 2 (Dai *et al*. 2022),

$$q_e = (C_O\text{-}C_e)\times V/m \quad (2)$$

where C_0 and C_e are the initial and equilibrium concentrations (mg/L) of Cu^{2+}, respectively; V is the volume (L) of the Cu^{2+} solution; and m is the mass (g) of the dried IPS_{gel}.

Adsorption isotherms

To better understand the interactions between the polymer network of IPS_{gel} and Cu^{2+}, adsorption experiments were conducted at pH 6 and 22 °C with initial Cu^{2+} concentrations of 25, 50, 75, 100, 125, 150, and 200 mg/L. The experimental data were then fitted with the Langmuir and Freundlich isotherm models. The Langmuir isotherm model (Langmuir 1933)describes monolayer adsorption on a homogeneous surface. In contrast, the Freundlich isotherm model (Azizian 2004)is used to evaluate adsorption on heterogeneous surfaces and is not restricted to monolayer adsorption. The linear forms of the Langmuir and Freundlich models are respectively presented in Eqs. 3 and 4.

Langmuir model:

$$C_e/q_e = C_e/q_{max} + 1/(K_L \cdot q_{max}) \quad (3)$$

Freundlich model:

$$\log q_e = 1/n \times \log C_e + \log K_F \quad (4)$$

In the isotherm equations, C_e is the equilibrium concentration of Cu^{2+} in solution (mg/L) and q_e is the adsorption capacity of IPS_{gel} at equilibrium (mg/g). The parameter q_{max} represents the maximum adsorption capacity. The parameter n is an empirical constant related to adsorption intensity in the Freundlich model. K_L is the Langmuir adsorption constant (L/mg), and K_F is the Freundlich capacity of the adsorbent (mg/g).

Adsorption kinetics

The adsorption kinetics of Cu^{2+} on IPS_{gel} were evaluated using the widely used pseudo-first-order and pseudo-second-order kinetic models. The kinetic experiments were conducted at pH 6.0 and 22 °C with an initial Cu^{2+} concentration of 100 mg/L. The pseudo-first-order and pseudo-second-order models (Ho and McKay 1999) are described by Eqs. 5 and 6:

Pseudo-first-order model:

$$\ln(q_e - q_t) = \ln q_e - k_1 \times t \quad (5)$$

Pseudo-second-order model:

$$t/q_t = 1/(k_2 \times q_e^2) + t/q_t \quad (6)$$

where q_e and q_t are the adsorption capacities at equilibrium (mg/g) and at time t (min), respectively. k_1 and k_2 are the rate constants of the pseudo-first-order (min^{-1}) and pseudo-second-order models (g/(mg·min)), respectively.

Desorption and regeneration studies

To evaluate the desorption efficiency of IPS_{gel}, samples were first immersed in a 100 mg/L Cu^{2+} solution until adsorption equilibrium was achieved. Then, these samples were subjected to desorption in 0.1 M HCl at 22 °C and 40 °C for 60 min. The desorption efficiency was calculated using Eq. 7,

$$E = (C_d \times V_d)/(q_e \times m) \times 100\% \quad (7)$$

where C_d is the concentration (mg/L) of Cu^{2+} in the HCl solution after desorption, V_d is the volume (L) of the desorption solution, m is the mass (g) of the adsorbent, and q_e is the equilibrium (mg/g) adsorption capacity for Cu^{2+} at an initial concentration of 100 mg/L.

To evaluate the reusability of IPS_{gel}, desorption was performed *via* immersion in 0.1 M HCl for 30 min, followed by regeneration using 0.1 M NaOH. The regenerated samples were washed with deionized water to a neutral pH and then dried before being reused in the subsequent adsorption cycle. The adsorption–desorption process was repeated for 20 cycles.

RESULTS AND DISCUSSION

Structural Characterization of IPS_{gel}

The synthesis route of IPS_{gel} is illustrated in Fig. 1(a). First, chitosan was treated *via* an alkaline dissolution method, followed by modification with hydrophobic isopropyl groups to obtain water-soluble IPS. This IPS was then employed as the sole gel framework to construct IPS_{gel} through covalent crosslinking.

The FTIR spectra of chitosan (CS) with a 95% degree of deacetylation, IPS, and IPS_{gel} are shown in Fig. 1(b). The broad peak at approximately 3390 cm^{-1} (Yan *et al.* 2017) was attributed to the stretching vibrations of the O–H and N–H groups in CS, IPS, and IPS_{gel}. In the FTIR spectra of IPS and IPS_{gel}, this peak was less intense than that of CS. The peaks at about 2889 and 2780 cm^{-1} (Liu *et al.* 2023) were ascribed to the stretching vibrations of alkyl C–H groups. The peak near 1590 cm^{-1} (Zhang *et al.* 2018) was associated with the bending vibration of the amide I band related to residual acetyl groups in chitosan. The peak at approximately 1368 cm^{-1} (Li *et al.* 2019) was assigned to the CH_2 wagging vibration at the C_6 position of the anhydroglucose unit. The peak at 1020 cm^{-1}

(Wang *et al.* 2018) was attributed to the asymmetric stretching vibration of the C–O–C group in the epoxy ring, confirming the successful formation of IPS_{gel}.

To investigate the thermoresponsive properties of IPS_{gel}, its volume changes at different temperatures were examined by observing its microstructural morphology under varying temperature conditions. Figure 1(c) shows SEM images of IPS_{gel} in the swollen state at 22 °C and the shrunken state at 40 °C. At 22 °C, IPS_{gel} exhibited an irregular and dense porous network structure with relatively numerous large pores. In contrast, raising the temperature to 40 °C induced noticeable volume shrinkage, leading to a more compact internal structure and a marked reduction in the number of large pores. These observations indicate that IPS_{gel} showed pronounced thermoresponsive swelling–shrinkage behavior.

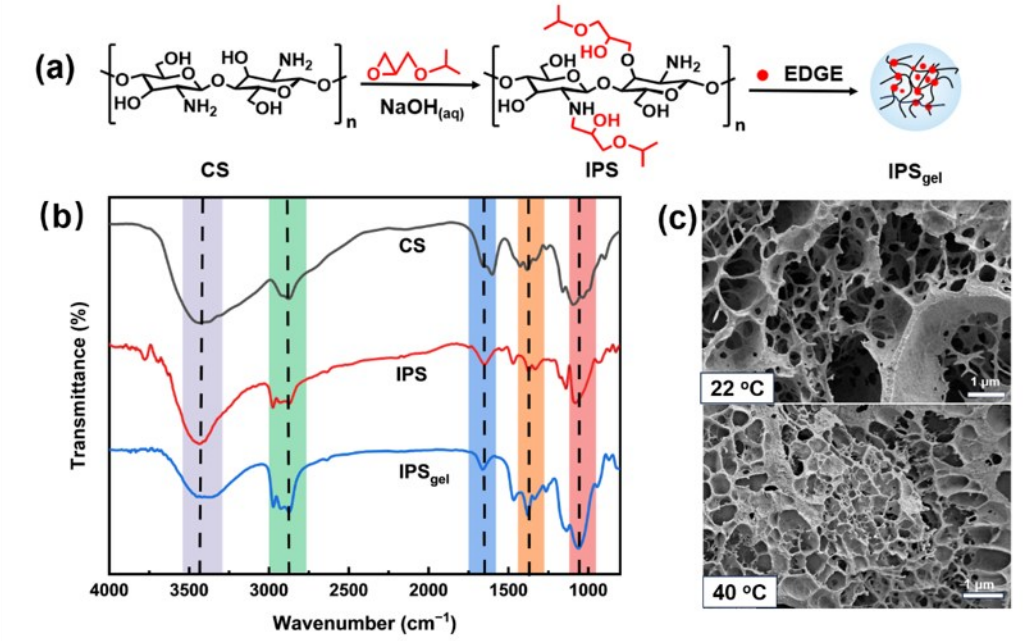

Fig. 1. (a) Synthesis schematic of IPS_{gel}; (b) FTIR spectra of CS, IPS, and IPS_{gel}; (c) SEM images of IPS_{gel} in the swollen state at 22 °C and in the shrunken state at 40 °C

Thermoresponsive Behavior of IPS_{gel}

The swelling ratio of IPS_{gel} over the temperature range of 21 to 48 °C was obtained to evaluate its VPTT and thermoresponsive behavior, as shown in Fig. 2(a). When the temperature was below the VPTT, the hydrophobic interactions of IPS were markedly weakened and hydrophilic interactions became dominant (Zha *et al*. 2026), resulting in increased water uptake and enhanced swelling. A sharp decrease in the swelling ratio was observed at approximately 35 °C, indicating the volume phase transition. Above 38 °C, the swelling ratio stabilized. When the temperature exceeded the VPTT, the hydrogen bonding interactions between water molecules and the IPS polymer chains were weakened, while hydrophobic interactions became dominant. This led to the shrinkage of the IPS_{gel} network and a reduction in pore size.

The effect of NaCl concentration (0, 4, 8, 12, and 20 g/L) on the VPTT of IPS_{gel} was investigated, as shown in Fig. 2(b). As the NaCl concentration increased, the equilibrium swelling ratio of IPS_{gel} markedly decreased. Despite the hydrophobic modification of IPS_{gel}, residual hydroxyl and amino groups remained on the polymer chains. The introduced Na^+ and Cl^- ions screened the electrostatic repulsion between these

charged groups, leading to polymer network contractions (Mussel *et al.* 2019). In addition, due to their strong hydration ability and ability to compete with polymer chains for water molecules, the salt ions disrupted the hydration shell of the hydrogel network (He *et al.* 2022). The presence of salt further weakens the interactions between water molecules and hydrophobic groups (such as isopropyl moieties) in thermoresponsive hydrogels, enhancing hydrophobic interactions. As a result, hydrogels undergo more pronounced shrinkage at lower temperatures or under the same temperature conditions (Sun *et al*. 2024; Zhou *et al.* 2025).

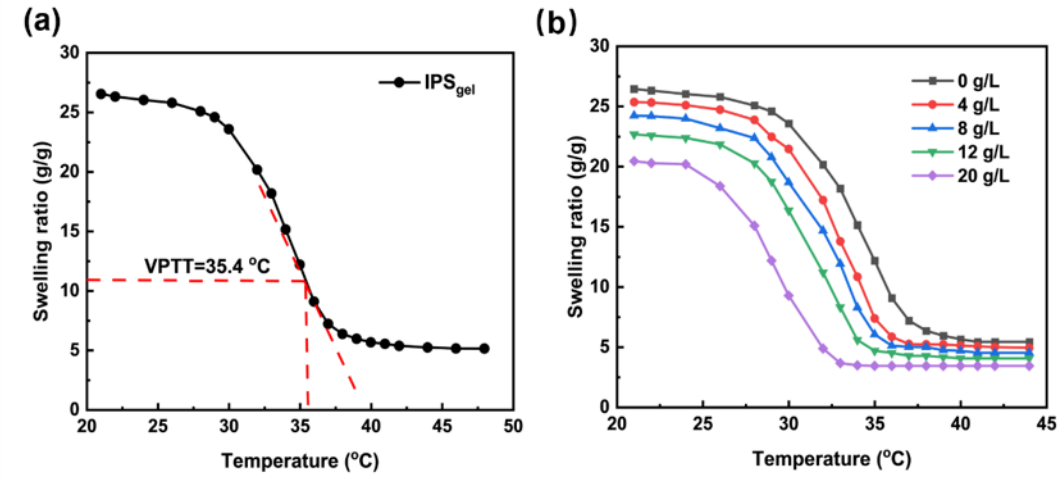

Fig. 2. (a) Equilibrium swelling ratio of IPS_{gel} as a function of temperature; (b) Effect of NaCl concentration (0, 4, 8, 12, 20 g/L) on the VPTT of IPS_{gel}

Cu^{2+} Adsorption Performance of IPS_{gel}

The adsorption performance of IPS_{gel} toward Cu^{2+} was investigated using initial Cu^{2+} concentrations of 25 to 200 mg/L. As shown in Fig. 3(a), the adsorption capacity rapidly increased at lower concentrations ($C_0 \leq 100$ mg/L) and then gradually approached a plateau as the initial concentration was further increased. At low Cu^{2+} concentrations, the rapid increase in adsorption capacity with increasing concentration can be attributed to the availability of abundant active binding sites on IPS_{gel}. However, at higher concentrations, the number of available binding sites becomes limited, and the complexation capacity of the functional groups is gradually saturated, resulting in a slower increase in adsorption capacity until equilibrium is reached (Yan *et al*. 2017).

The pH value, which influences both the speciation of copper ions in solution and the physicochemical properties of the hydrogel adsorbent (Jung *et al.* 2022), is a key factor affecting the adsorption of Cu^{2+} by IPS_{gel}. The effect of pH on the adsorption capacity of IPS_{gel} is shown in Fig. 3(b). At pH values below 3.5, IPS_{gel} showed a relatively low adsorption capacity for Cu^{2+}. This behavior is likely due to the protonation of amino groups on the IPS_{gel} surface, particularly those not involved in crosslinking. Protonation results in electrostatic repulsion between positively charged Cu^{2+} and the hydrogel surface as well as the competitive occupation of active sites by H^+, inhibiting adsorption (Moralez *et al.* 2025). However, when the pH was raised above 3.5, the concentration of H^+ decreased, reducing this competitive effect and enhancing Cu^{2+} adsorption. As a result, the adsorption capacity rapidly increased. At pH 6.0, IPS_{gel} exhibited a maximum adsorption capacity of 24.5 mg/g.

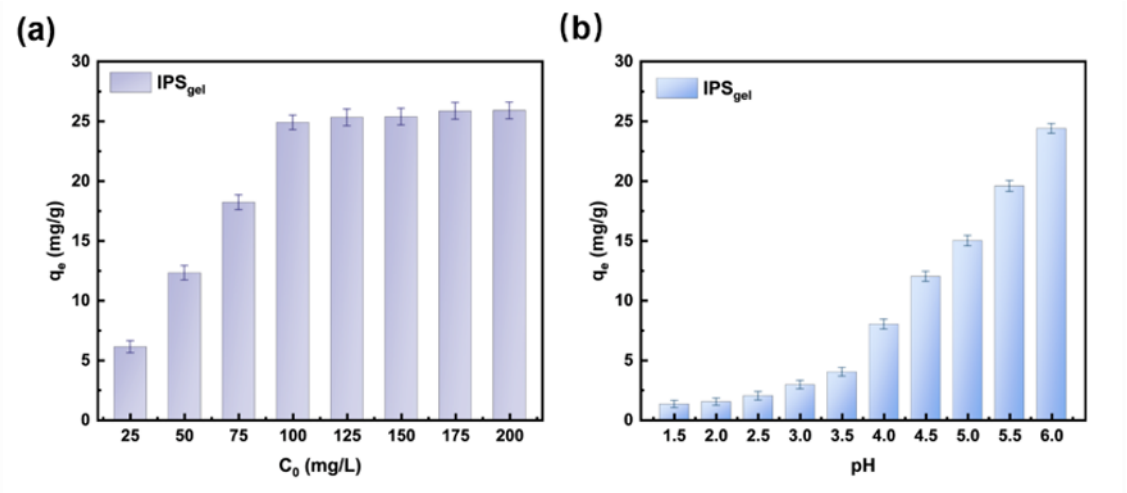

Fig. 3. (a) Effect of initial Cu^{2+} concentration on adsorption capacity of IPS_{gel} (C_0 = 25 to 200 mg/L, T = 22 °C); (b) Effect of solution pH on Cu^{2+} adsorption efficiency of IPS_{gel} (C_0 = 100 mg/L, T = 22 °C)

Adsorption Isotherms and Kinetics

To better understand the interaction between the IPS_{gel} polymer network and Cu^{2+}, the adsorption data were fitted using the Langmuir and Freundlich models to describe the variation of adsorption capacity with concentration (Xu *et al.* 2025). The Langmuir isotherm which assumes monolayer adsorption on a uniform surface, provided a better fit (R^2 = 0.989) than the Freundlich model (R^2 = 0.974), as shown in Fig. 4(a). The excellent fits to both models suggests that the Cu^{2+} adsorption on IPS_{gel} was predominantly monolayer in nature.

The adsorption kinetics were further evaluated to understand the Cu^{2+} adsorption rate. As shown in Fig. 4(b), the experimental data were fitted with both the pseudo-first-order (R^2 = 0.987) and pseudo-second-order (R^2 = 0.990) kinetic models, both of which provided satisfactory mathematical descriptions of the adsorption process. The adsorption of Cu^{2+} proceeded rapidly and approached a plateau within 60 min, reaching equilibrium at approximately 120 min with an equilibrium adsorption capacity of 24.5 mg/g (Ofomaja *et al*. 2010).

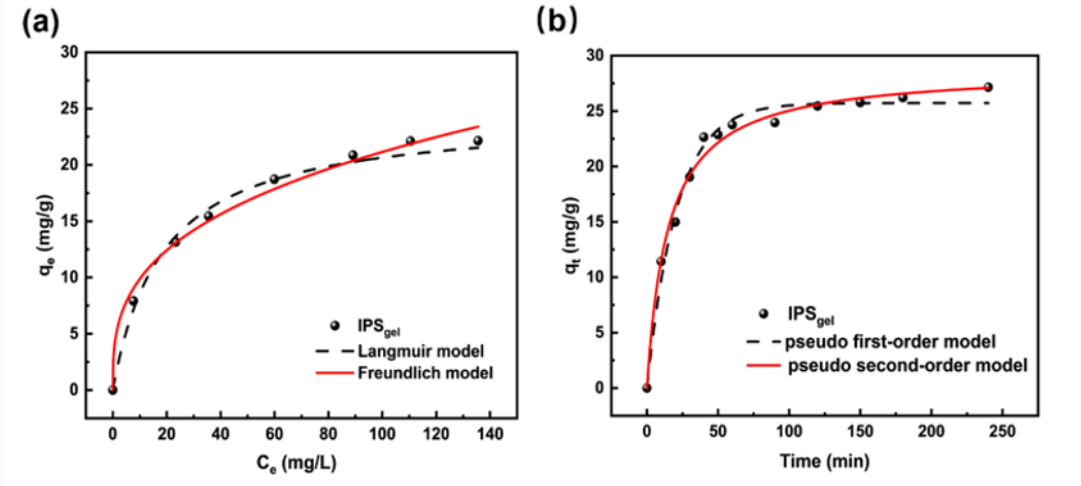

Fig. 4. (a) Adsorption isotherm of Cu^{2+} on IPS_{gel} (C_0 = 100 mg·L^{-1}, *T* = 22 °C, pH = 6); (b) Adsorption kinetics of Cu^{2+} on IPS_{gel} (C_0 = 100 mg·L^{-1}, *T* = 22 °C, pH = 6)

Table 1. Isotherm Parameters for Cu^{2+} Adsorption onto IPS_{gel}

Langmuir Model			Freundlich Model		
R^2	q_{max} (mg/g)	K_L (L/mg)	R^2	n	K_F ($mg^{1-n} \cdot L^n/g$)
0.989	24.5	0.054	0.974	4.60	0.331

Table 2. Kinetic Parameters for Cu^{2+} Adsorption onto IPS_{gel}

Pseudo-first-order Model			Pseudo-second-order Model		
R^2	q_1 (mg/g)	K_1 (min^{-1})	R^2	$q_{e,c}$ (mg/g)	K_2 (g/(mg·min))
0.987	25.7	0.047	0.990	28.8	0.002

Regeneration and Reusability of IPS_{gel}

In conventional adsorbent systems, the desorption and regeneration of the adsorbent material typically require large amounts of acid, alkali, or other eluents, which increases operational costs and may also cause secondary environmental pollution. As shown in Fig. 5(a), IPS_{gel} in the shrunken and swollen states was immersed in a volume of 0.1 M HCl solution for desorption. At 40 °C, the IPS_{gel} contracted, expelled a large amount of water, and exhibited a noticeable reduction in volume. Consequently, compared with the swollen state, the shrunken state required substantially less HCl for effective desorption. As illustrated in Fig. 5(b), the desorption efficiency of IPS_{gel} in the shrunken state reached 83% within 50 min, while a desorption efficiency of only 66% was achieved in the swollen state over the same period, indicating markedly enhanced desorption performance under the shrunken condition (Cai *et al.* 2021; Wen *et al.* 2022).

Reusability is also a key aspect of practical adsorption applications. Therefore, adsorption–desorption cycling experiments were conducted to evaluate the regeneration performance of IPS_{gel}. As shown in Fig. 5(c), after 20 cycles, the adsorption capacity of IPS_{gel} slightly decreased from 25.6 mg/g to 22.3 mg/g, demonstrating a capacity retention of 86.9%. These results demonstrate that IPS_{gel} possesses excellent regeneration properties and shows strong potential for heavy metal removal in wastewater treatment applications.

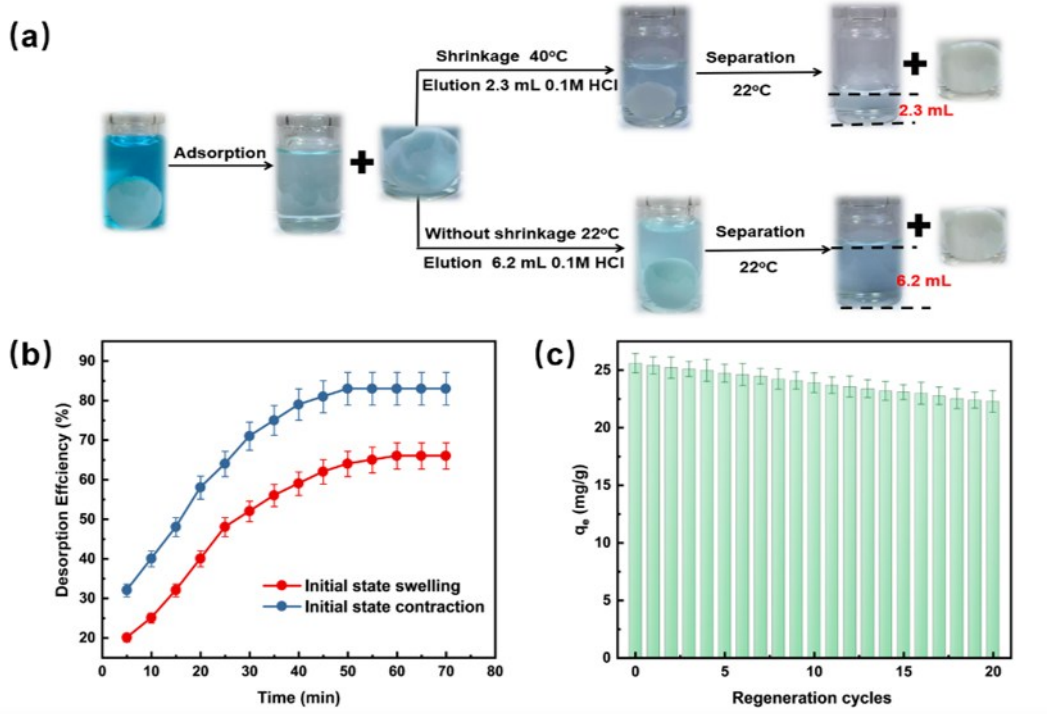

Fig. 5. (a) Elution efficiency comparison of Cu^{2+}-loaded IPS_{gel} under swollen (22 °C) and shrunken (40 °C) states; (b) Desorption efficiency of IPS_{gel} under swollen and shrunken states within 70 min; (c) Adsorption capacity of IPS_{gel} after 20 adsorption cycles

CONCLUSIONS

1. IPS_{gel} exhibited the adsorption capacity of 24.5 mg/g for Cu^{2+}, and its adsorption performance was influenced by solution pH and initial Cu^{2+} concentration; the adsorption isotherm followed the Langmuir model, and the kinetics followed the pseudo-second-order model.
2. The Cu^{2+}-loaded IPS_{gel} could be effectively regenerated using a small amount of HCl solution, representing an 88 to 95% reduction in acid consumption compared to conventional hydrogels; even after 20 adsorption–desorption cycles, IPS_{gel} maintained good adsorption performance.
3. IPS_{gel} is a thermoresponsive, high-capacity chitosan-based adsorbent that enables efficient Cu^{2+} removal and low-acid regeneration, unlike conventional adsorbents requiring high acid consumption, thereby providing a green strategy and showing promise for Cu^{2+} removal from wastewater.

ACKNOWLEDGMENTS

The authors are grateful for the support of the National Natural Science Foundation of China (Nos. 22278062, 31901775); Dalian, Science and Technology Innovation Fund (2024JJ13GX047); Liaoning Provincial (2025-MSLH-126).

REFERENCES CITED

Arafa, E. G., Mahmoud, R., Gadelhak, Y., and Gawad, O. F. A. (2024). "Design, preparation, and performance of different adsorbents based on carboxymethyl chitosan/sodium alginate hydrogel beads for selective adsorption of Cadmium (II) and Chromium (III) metal ions," *International Journal of Biological Macromolecules* 273, article 132809. https://doi.org/10.1016/j.ijbiomac.2024.132809

Azizian, S. (2004). "Kinetic models of sorption: A theoretical analysis," *Journal of Colloid and Interface Science* 276(1), 47-52. https://doi.org/10.1016/j.jcis.2004.03.048

Badsha, M. A. H., Khan, M., Wu, B. L., Kumar, A., and Lo, I. M. C. (2021). "Role of surface functional groups of hydrogels in metal adsorption: From performance to mechanism," *Journal of Hazardous Materials* 408, article 124463. https://doi.org/10.1016/j.jhazmat.2020.124463

Cai, L. Q., Ying, D. F., Liang, X. C., Zhu, M. X., Lin, X. H., Xu, Q., Cai, Z. W., Xu, X. J., and Zhang, L. N. (2021). "A novel cationic polyelectrolyte microsphere for ultrafast and ultra-efficient removal of heavy metal ions and dyes," *Chemical Engineering Journal* 410, article 1128404. https://doi.org/10.1016/j.cej.2021.128404

Cai, Y., Fang, M., Tan, X., Hu, B., Wang, X. J. S., and Technology, P. (2024). "Highly efficient selective elimination of heavy metals from solutions by different strategies," *Separation and Purification Technology* 350, article 127975. https://doi.org/10.1016/j.seppur.2024.127975

Chen, J. J., Wang, X. H., Huang, X. Y., Tong, Z. L., Zhou, J. Y., Shen, Y. T., and Hao, C. (2025). "Construction of cellulose-based hydrogel compounded with modified kaolin and its removal performance for heavy metal ions and dyes in water," *International Journal of Biological Macromolecules* 306, article 141398. https://doi.org/10.1016/j.ijbiomac.2025.141398

Chen, X. Q., Song, Z. H., Yuan, B. N., Li, X. J., Li, S. P., Nguyen, T. T., Guo, M. H., and Guo, Z. H. (2022). "Fluorescent carbon dots crosslinked cellulose nanofibril/chitosan interpenetrating hydrogel system for sensitive detection and efficient adsorption of Cu (II) and Cr (VI)," *Chemical Engineering Journal* 430, article 133154. https://doi.org/10.1016/j.cej.2021.133154

Crini, G., and Lichtfouse, E. (2019). "Advantages and disadvantages of techniques used for wastewater treatment," *Environmental Chemistry Letters* 17(1), 145-155. https://doi.org/10.1007/s10311-018-0785-9

Dai, M. Y., Zhang, Y. D., Zhang, L. P., Tian, Y., Liu, G., Zhao, J., Liu, Y., Zhu, S. M., and Ye, Z. Y. (2022). "Multipurpose polysaccharide-based composite hydrogel with magnetic and thermoresponsive properties for phosphorus and enhanced copper (II) removal," *Composites Part A: Applied Science and Manufacturing* 157, article 106916. https://doi.org/10.1016/j.compositesa.2022.106916

De Luna, M. D. G., Flores, E. D., Cenia, M. C. B., and Lu, M. C. (2015). "Removal of copper ions from aqueous solution by adlai shell (*Coix lacryma-jobi* L.) adsorbents," *Bioresource Technology* 192, 841-844. https://doi.org/10.1016/j.biortech.2015.06.018

He, Q., Fang, Y. Q., Han, Y., Qin, W. N., Nie, J. K., Hou, D., and Zhu, K. J. (2022). "Novel synthesis of PVA/NaCl hydrogel for reversible thermochromism," *Bioresource Technology* 132, article 112754. https://doi.org/10.1016/j.optmat.2022.112754

Ho, Y. S., and McKay, G. (1999). "Pseudo-second order model for sorption processes," *Process Biochem.* 34(5), 451-465. DOI: 10.1016/S0032-9592(98)00112-5

Jeremias, J. S. D., Lin, J. Y., Dalida, M. L. P., and Lu, M. C. (2023). "Abatement technologies for copper containing industrial wastewater effluents – A review," *Journal of Environmental Chemical Engineering* 11(2), article 109336. https://doi.org/10.1016/j.jece.2023.109336

Jung, M. J., Kim, J. K., Jung, S. G., Kim, Y. J., Bang, J. S., Yeo, H. Y., Choi, I. G., and Kwak, H. W. (2022). "pH-responsive hydrogels of carboxymethyl cellulose and polyethyleneimine for efficient removal of ionic dye molecules," *BioResources* 17(4), 5785-5802. https://doi.org/10.15376/biores.17.4.5785-5802

Ofomaja, A. E., Naidoo, E. B., and Modise, S. J. (2010). "Dynamic studies and pseudo-second order modeling of copper(II) biosorption onto pine cone powder," *Desalination* 251(1–3), 112-122. https://doi.org/10.1016/j.desal.2009.09.135

Khan, M. N., Chowdhury, M., and Rahman, M. M. (2021). "Biobased amphoteric aerogel derived from amine-modified clay-enriched chitosan/alginate for adsorption of organic dyes and chromium (VI) ions from aqueous solution," *Materials Today Sustainability* 13, article 100077. https://doi.org/10.1016/j.mtsust.2021.100077

Langmuir, I. (1933). "Surface chemistry," *Chemical Reviews* 13(2), 147-191. https://doi.org/10.1021/cr60045a001

Li, W., Ju, B., and Zhang, S. (2019). "Preparation of cysteamine-modified cellulose nanocrystal adsorbent for removal of mercury ions from aqueous solutions," *Cellulose* 26(8), 4971-4985. https://doi.org/10.1007/s10570-019-02420-1

Liu, F., Wang, L., Zhai, X., Ji, S., Ye, J., Zhu, Z., Teng, C., Dong, W., and Wei, W. (2023). "A multi-functional double cross-linked chitosan hydrogel with tunable mechanical and antibacterial properties for skin wound dressing," *Carbohydrate Polymers* 322, article 121344. https://doi.org/10.1016/j.carbpol.2023.121344

Moralez, L., Nakasu, P., and Hallett, J. (2025). "Preparation of hybrid β-chitosan–squid pen protein hydrogel beads by ionic liquid regeneration for adsorption of copper (ii) and zinc (ii) from wastewater," *Soft Matter* 21(13), 2480-2492. https://doi.org/10.1039/d4sm01300j

Mussel, M., Basser, P. J., and Horkay, F. (2019). "Effects of mono-and divalent cations on the structure and thermodynamic properties of polyelectrolyte gels," *Soft Matter* 15(20), 4153-4161. https://doi.org/10.1039/c9sm00464e

Nankawa, T., Sugita, A., Fukakusa, C., Yamada, T., and Sekine, Y. (2025). "Freeze-crosslinked biomass-based chitosan sponge hydrogels with metal-induced mechanical enhancement for high-performance Cu^{2+} and Pb^{2+} adsorption," *Separation and Purification Technology* 378, article 134780. https://doi.org/10.1016/j.seppur.2025.134780

Park, S. H., and Lee, S. J. (2022). "Thermoresponsive Al^{3+}-crosslinked poly(N-isopropylacrylamide)/alginate composite for green recovery of lithium from Li-spiked seawater," *Green Energy & Environment* 7(2), 334-344. https://doi.org/10.1016/j.gee.2020.10.006

Sahu, P., Patel, A. R., Pandey, A., Hait, M., and Patra, G. K. (2025). "Assessment of heavy metal ion toxicity in wastewater: A comprehensive review," *Inorganica Chimica Acta* 585, article 122751. https://doi.org/10.1016/j.ica.2025.122751

Suljovrujic, E., Miladinovic, Z. R., Micic, M., Suljovrujic, D., and Milicevic, D. (2019). "The influence of monomer/solvent feed ratio on POEGDMA thermoresponsive hydrogels: Radiation-induced synthesis, swelling properties and VPTT," *Radiation Physics and Chemistry* 158, 37-45. https://doi.org/10.1016/j.radphyschem.2018.12.034

Sun, M., Sun, H., Wei, R., Li, W., Lai, J., Tian, Y., and Li, M. (2024). "Energy-efficient smart window based on a thermochromic hydrogel with adjustable critical response temperature and high solar modulation ability," *Gels* 10(8), article 494. https://doi.org/10.3390/gels10080494

Wang, C., Sun, M., Zha, X., Meng, Z., Ye, Y., Sun, H., Liu, Y., Ju, B., and Tian, Y. (2025). "Bidirectional thermoresponsive window *via* a facilely tailorable double-layer hydrogel," *ACS Applied Materials and Interfaces* 17(52), 70887-70898. https://doi.org/10.1021/acsami.5c19264

Wang, Y. Q., Feng, Y., Zhang, X. F., Zhang, X. G., Jiang, J. L., and Yao, J. F. (2018). "Alginate-based attapulgite foams as efficient and recyclable adsorbents for the removal of heavy metals," *Journal of Colloid and Interface Science* 514, 190-198. https://doi.org/10.1016/j.jcis.2017.12.035

Wen, H., Soyekwo, F., and Liu, C. K. (2022). "Highly permeable forward osmosis membrane with selective layer 'hooked' to a hydrophilic Cu-alginate intermediate layer for efficient heavy metal rejection and sludge thickening," *Journal of Membrane Science* 647, article 120247. https://doi.org/10.1016/j.memsci.2021.120247

Xu, M. X., Zhu, H. Y., Miao, T., Liu, X. Q., Zhang, H. P., Lian, Y. K., Tang, H. M., and Cheng, Z. X. (2025). "Statistical interpretation of Langmuir-Freundlich equation for physical adsorption by exchange-electron number of adsorbate with surface," *Separation and Purification Technology* 373, article 133501. https://doi.org/10.1016/j.seppur.2025.133501

Yan, Y. Z., An, Q. D., Xiao, Z. Y., Zheng, W., and Zhai, S. G. (2017). "Flexible core-shell/bead-like alginate@PEI with exceptional adsorption capacity, recycling performance toward batch and column sorption of Cr(VI)," *Chemical Engineering Journal* 313, 475-486. https://doi.org/10.1016/j.cej.2016.12.099

Zha, X., Wang, C., Meng, Z., Ye, Y., Sun, H., Tan, C., and Tian, Y. (2026). "Intrinsically thermoresponsive hydrogels from molecularly engineered chitosan," *Gels* 12(2), article 119. https://doi.org/10.3390/gels12020119

Zhang, Y., Lin, S., Qiao, J., Kołodyńska, D., Ju, Y., Zhang, M., Cai, M., Deng, D., and Dionysiou, D. D. (2018). "Malic acid-enhanced chitosan hydrogel beads (mCHBs) for the removal of Cr (VI) and Cu (II) from aqueous solution," *ACS Sustainable Chemistry* 353, 225-236. https://doi.org/10.1016/j.cej.2018.06.143

Zhen, Y., Ge, L., Chen, Q., Xu, J., Duan, Z., Loor, J. J., Wang, M. Z. (2022). "Latent benefits and toxicity risks transmission chain of high dietary copper along the livestock–environment–plant–human health axis and microbial homeostasis: A review," *Journal of Agricultural and Food Chemistry* 70(23), 6943-6962. https://doi.org/10.1021/acs.jafc.2c01367

Zhi, J. H., Bai, X. L., Wang, Q. Y., Wang, T. T., Verma, Y., Sharma, G., Kumar, A., and Dhiman, P. (2025). "Natural gums-derived hydrogels for adsorptive removal of heavy metals: A review," *International Journal of Biological Macromolecules* 310, article 143350. https://doi.org/10.1016/j.ijbiomac.2025.143350

Zhou, Y., Xie, Z., Wu, F., Qin, J., Zhang, X., Zhang, J., Ma, X., Fan, L., Wang, X., Wang, J. J. R., *et al*. (2025). "Facile fabrication and characterization of double network starch/PVA/NaCl composite hydrogel for flexible strain sensor," *Reactive and Functional Polymers* 208, article 106163. https://doi.org/10.1016/j.reactfunctpolym.2025.106163

Article submitted: April 16, 2026; Peer review completed: May 9, 2026; Revisions accepted: June 19, 2026; Published: July 10, 2026.
DOI: 10.15376/biores.21.3.8001-8014